

Cite this: *J. Mater. Chem.*, 2011, **21**, 16057

www.rsc.org/materials

PAPER

## A highly practical route for large-area, single layer graphene from liquid carbon sources such as benzene and methanol†

Srinivas Gadipelli,<sup>ab</sup> Irene Calizo,<sup>b</sup> Jamie Ford,<sup>ab</sup> Guangjun Cheng,<sup>b</sup> Angela R. Hight Walker<sup>b</sup> and Taner Yildirim<sup>\*ab</sup>

Received 24th June 2011, Accepted 16th August 2011

DOI: 10.1039/c1jm12938d

Through a detailed systematic study, we determined the parameters critical for high-quality, single-layer graphene formation and developed a straightforward synthesis that requires no explosive hydrogen or methane gas flow. The synthesis is further simplified by using only a liquid carbon source such as methanol. Of over a dozen liquid carbon sources studied, methanol is found to be unique in that it acts as both a carbon/hydrogen source and an inhibitor to amorphous carbon growth. No deposition of amorphous carbon was observed, regardless of vapor pressure, unlike methane and other hydrocarbons. Finally, we describe a protocol to control graphene growth to a single side or selected location on the copper substrate, which is required for most device applications. Using our novel methods, we have prepared high-quality, single-layer graphene samples at the inch scale that have been thoroughly characterized with Raman spectroscopy, optical transmittance, scanning electron microscopy and sheet resistance measurements. Our method is safe, simple, and economical and will be of value to both fundamental researchers and nanodevice engineers.

### Introduction

Graphene research is extremely active due to its extraordinary mechanical, optical, and electronic properties.<sup>1–5</sup> In order to realize the remarkable properties of graphene in practical electronic devices, a safe, scalable, and inexpensive synthesis method is necessary. The growth of graphene (which was originally known as “monolayer graphite (MG)”<sup>6</sup>) on metal surfaces goes back as early as 1969.<sup>6–10</sup> In these early studies, MG growth by pyrolysis of small hydrocarbons, such as acetylene over metals as well as the dissolution-precipitation of carbon in various metals was observed<sup>6–10</sup> and reviewed.<sup>11</sup> However, real interest in graphene developed with the report of isolated graphene films in 2004.<sup>2</sup> This work was based on micromechanical cleavage of graphite that produced only small area films on the order of tens of micrometres and was not scalable. Recently, many different synthesis methods have been reported.<sup>12–25</sup> These include carbon segregation from silicon carbide or metal substrates following high temperature annealing and chemical vapor deposition

(CVD) of hydrogen and methane over various metal foils at high temperatures.<sup>12–14</sup> Very recently graphene growth from solid carbon sources has been also demonstrated.<sup>21</sup> The CVD method is currently the most promising as it enables synthesis of large-area, high-quality, single-layer graphene. In particular, Ruoff *et al.*<sup>15,16</sup> reported the CVD synthesis of large-area graphene on copper foils by taking advantage of the low carbon solubility in copper. Using PMMA films to transfer the graphene to other substrates, they started a new era in graphene synthesis for practical applications.<sup>17</sup>

There are drawbacks to CVD synthesis, such as the need for large amounts of explosive gas (H<sub>2</sub> and CH<sub>4</sub>) and expensive furnaces and flow controllers. Consequently, it is important to establish alternative methods to grow large-area, single-layer graphene that are safe, simple and can be carried out in an ordinary research laboratory. In this article, we discuss our systematic study of the parameters that are critical for high-quality, single-layer graphene formation. Our results not only shed light on the graphene growth mechanism, but have also yielded a straightforward synthesis method that requires neither H<sub>2</sub>/CH<sub>4</sub> flow nor any specialized CVD equipment. We also present a simple method to ensure the graphene grows only on one side and/or selected location of a copper foil, which is required for patterned graphene growth for device applications. Using our novel protocol, we have prepared high-quality, single-layer graphene samples at the inch scale that have been fully characterized by Raman spectroscopy, optical transmittance, scanning electron microscopy and sheet resistance measurements. Since our method is safe, simple and

<sup>a</sup>National Institute of Standards and Technology, Gaithersburg, Maryland MD, 20899, USA. E-mail: taner@seas.upenn.edu; Fax: +301-9219847; Tel: +301-9756228

<sup>b</sup>Department of Materials Science and Engineering, University of Pennsylvania, Philadelphia, PA, 19104, USA

† Electronic supplementary information (ESI) available: The details of graphene growth process and transfer, the Raman plots from as-grown copper-graphene foils from different liquid-carbon sources are given in supporting information. See DOI: 10.1039/c1jm12938d

inexpensive, it will be of great value both for fundamental research and practical applications that require practical synthesis of high-quality, large-area graphene films.

## Experimental section

### Graphene synthesis

A schematic view of our setup for static and dynamic exposure of hydrocarbon vapors is shown in Fig. 1 a-b. Figures of the experimental setup are shown in supporting information (ESI†), Fig. S1. For methane, a small stainless steel tube with VCR fittings was filled with 1–5 atm methane using a Sievert type apparatus.<sup>33</sup> A small amount of methane vapor was then introduced into the system through a needle valve. For liquid carbon sources, we filled a small glass tube (6 and ~4 mm outer and inner diameters – ~85 mm liquid height corresponds to 1 cc liquid) and connected it to the needle valve as shown in Fig. S1b.† Methanol and ethanol were dried with 3 Å molecular sieves and degassed prior to experiments. All other liquid carbon sources such as benzene were used as received.

Since hydrogen is not used prior to graphene growth, it is important that the copper foil is pre-cleaned with acid. Cleaning with either 5 wt% (4 : 1 HNO<sub>3</sub>/HCl) acid solution or acetic acid cleaning yielded similar results. Copper foils that were not

pre-cleaned also yielded graphene but with poorer coverage and lower quality graphene than on pre-cleaned foils. The copper foils were first degreased with acetone, washed with DI water, sonicated in 5 wt% (4 : 1 HNO<sub>3</sub>/HCl), washed with DI water and acetone, and then dried with nitrogen. The main effect of cleaning is not to remove the surface oxygen but to remove the grease and other contaminants that could deposit carbon at high temperature, yielding amorphous carbon or multilayer graphene with defects. In particular, when the Cu foil or the quartz-tube are not cleaned properly, we have observed partial graphene formation on copper foil after annealing even without exposing any gases or liquids. Therefore, we always preheat the quartz-tube at 900 °C in air for several minutes to make sure all residual carbon on the tube are burned out. The copper foil is slowly heated to make sure the residual solvent left on the surface are evaporated before copper annealing procedure at 900–1000 °C.

For a typical synthesis, we rolled a 1 × 3 inch copper foil into a cylinder, placed it in a one inch ID quartz tube and then evacuated the system to base pressure (~1 × 10<sup>-4</sup> torr) (see Fig. S1, ESI†). Then we heated copper foil/tube to 900–1000 °C for one hour. Longer annealing, up to 12 h, did not affect the resulting graphene. After the annealing, the desired dose of a given hydrocarbon was introduced for 5–10 min. Longer exposures and high pressures lead to low-quality graphene or amorphous carbon films. We typically use less than 0.05 cc of

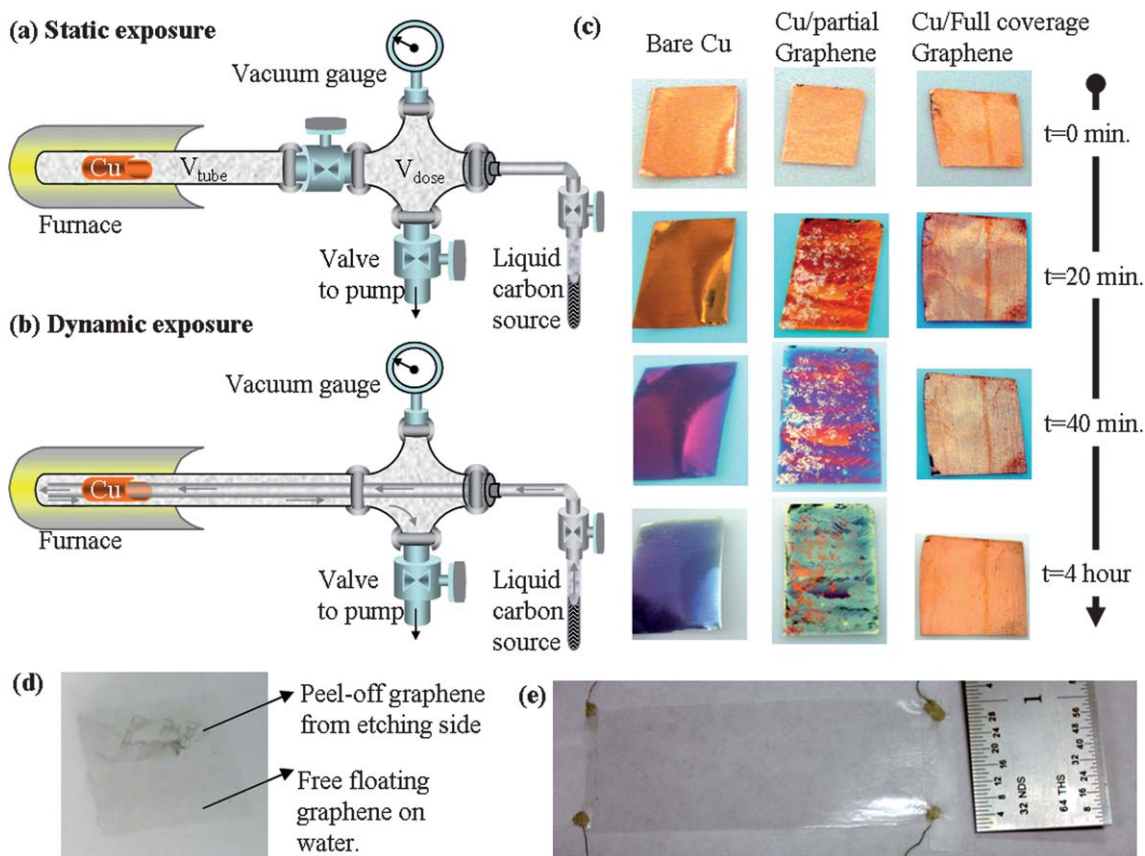


**Fig. 1** Schematic view of the experimental setup for graphene synthesis using static (a) and dynamic (b) exposure of methane or liquid hydrocarbon vapor as a carbon source. (c) Oxidation of copper foils at 170 °C as a function of time and graphene coverage. Note that the fully coated graphene copper foil does not show any oxidation with visual inspection. (d) Free floating graphene film with a second sheet from the etched underside. (e) Large scale (1 × 3 inch<sup>2</sup>) PMMA/Graphene film synthesized from methanol, showing ~550 Ohm/□ sheet resistance.

liquid carbon source. We calibrate the flow-rate by pumping the system for an hour and measuring the decrease in the level of liquid carbon source. We used 3 mm OD glass tube which has about 1 cc volume with 90 mm liquid height. Hence, in a typical experiment of 10 min. exposure, one usually does not notice the drop in the liquid level. If too much liquid is used, we observe either amorphous carbon films or graphene with very large defect peak in the Raman spectra.

After the exposure, the carbon source is closed and the system is evacuated for five to ten minutes at 1000 °C until base vacuum pressure is reached. Then, the tube is removed and air quenched. We found that cooling rate had no effect on the graphene films (see Fig. S3, ESI†).

### Graphene transfer

In order to characterize our graphene samples, we transferred the graphene films from copper to different substrates with the poly-methyl methacrylate (PMMA) support-film method.<sup>16</sup> Briefly, as-grown graphene films on copper were spin-coated with PMMA at 500 rpm for 5 s and 3000 rpm for 45 s. The PMMA-coated Cu foils were baked at 170 °C for 5 min and etched with 1 M FeCl<sub>3</sub> solution. After complete removal of the copper substrate, the FeCl<sub>3</sub> solution were first replaced with 5 wt% HCl solution (to remove the residual copper and FeCl<sub>3</sub>) and then DI water using a syringe several times and then the PMMA/graphene film were transferred to a large DI-water bath. The target substrate was then manually inserted underneath the floating film, completing transfer. After the film dried, we annealed it in vacuum furnace at 170 °C for 30 min to relax the PMMA film. This minimized cracking of the graphene film during PMMA removal. The PMMA support films were easily removed with acetic acid, followed by an acetone wash and drying under nitrogen flow. Fig. 7 show various large-area transferred graphene films and the corresponding Raman spectra. The spatially resolved Raman scans and optical images show that the transfer of graphene films were successful and the samples contain mainly single layer graphene.

### Characterization

**Raman measurements.** Raman spectra were acquired under ambient conditions with a Renishaw InVia micro-Raman spectrometer equipped with a 514 nm (2.41 eV) wavelength excitation laser and an 1800 lines/mm grating while operated in 180° backscattering geometry. A 50x objective was used to focus the excitation laser light spot of approximately 2 microns on the graphene samples with an on-sample incident power of less than 2 mW to avoid local heating effects.

**Mass spectroscopy measurements.** The mass spectroscopy experiments were performed with a Pfeiffer Vacuum Thermostar mass spectrometer (MS) connected to a TA Instruments Q600 Simultaneous Thermogravimetric Analyzer/Differential Scanning Calorimeter (SDT). CeO<sub>2</sub> or Cu powder were loaded into an alumina pan in the SDT and purged with helium flowing at 100 mL/min. The methanol vapor was introduced into the auxiliary inlet of the SDT by flowing He through a methanol bubbler at 0.2 cubic feet per minute. When the MS signal for

methanol stabilized ( $m/z = 31$  and  $32$ ), the SDT was heated from 30 to 1000 °C at 20 °C/min. MS data for  $m/z = 2$  (H<sub>2</sub>), 4 (He), 15 (CH<sub>4</sub>), 16 (CH<sub>4</sub>), 18 (H<sub>2</sub>O), 28 (CO), 31 (CH<sub>3</sub>OH), and 32 (CH<sub>3</sub>OH) were recorded continuously during the heating cycle.

**SEM measurements.** Scanning electron microscopy (SEM) of the graphene samples was performed using a Zeiss Ultra-60 field emission SEM. Data shown here were obtained with a 1 kV incident electron energy and in-lens detector at 5 mm working distance.

## 3. Results and discussion

Even though the mechanism of CVD graphene formation were extensively studied as a function of hydrogen annealing and methane flow rate,<sup>12–14</sup> to the best of our knowledge there is no study to show that such high flow rates are actually necessary for graphene formation. Hence, we first investigated whether or not the large amounts of hydrogen and methane typically used in CVD synthesis<sup>13</sup> is necessary for graphene formation. While high flow rates are important for gram-scale synthesis of fullerenes and nanotubes, it may not be required for a one-atom thick layer of carbon. We designed a simple apparatus to test the need for H<sub>2</sub>/CH<sub>4</sub> flow, shown in Fig. 1a-b. Pictures of the actual setup and the details of the sample preparation protocol are given in the supporting information and methods. Briefly, our experimental setup enables the copper substrate to be heated under vacuum and then exposed to a given pressure of methane or other liquid hydrocarbon vapors with or without vapor flow. For static exposure, we fill the dosing volume with a given pressure of carbon-source and then open the sample valve to expose the vapor to the hot copper foil for a given exposure time. During this process, we do not flow any gas. For the dynamic exposure shown in Fig. 1b, we constantly pump the system from one end and leak the carbon-source vapor through a needle valve at the other end. By monitoring the liquid level in the reservoir, we determined the flow-rate, typically 0.06 cc/h. We systematically varied the temperature, duration of vapor exposure, and pressure to determine the best conditions for uniform, single-layer graphene formation.

Leveraging several screening tests, a given set of parameters were optimized for graphene production. In order to ascertain if the copper foil is coated with graphene and/or some form of carbon, the oxidation of the foils in air at 170 °C was monitored as a function of time. As shown in Fig. 1c, bare copper foil oxidizes very rapidly, exhibiting changing and uniform colors with increasing copper oxide film on the surface. On the other hand, partially coated graphene/copper sample (middle panel) shows non-uniform oxidization. Interestingly, fully-coated, graphene-copper samples show no sign of oxidization for up to 12 h with visual inspection. This may be expected if the copper surface is protected from oxygen by the graphene layer, although quantitative measurements are necessary to determine this for certain. This is the easiest and quickest check of successful synthesis. It also suggests that graphene on metal surfaces could be used as a high-temperature, oxidization-resistance coating for protection against corrosion and other external chemical agents. As a second screening check, we etched the copper foils with 1 M FeCl<sub>3</sub> solution. Uniform graphene samples yielded robust,

transparent graphene films, while partially formed graphene films collapsed or broke into pieces during etching. We also note that uniform graphene samples formed a second peel-off graphene layer from the underside of the Cu foil that needs to be carefully removed; otherwise the resulting graphene film would have random regions with multiple graphene layers. Amorphous carbon samples showed dark gray films that broke easily when touched.

Micro-Raman spectroscopy is a well established method of identifying the number of graphene layers on micro-mechanically exfoliated graphene.<sup>22–24</sup> The most intense features in the Raman spectrum of graphene are the G ( $\approx 1580\text{ cm}^{-1}$ ) and the G' or 2D ( $\approx 2700\text{ cm}^{-1}$ ) bands. Typically, the ratio of their intensities and the 2D bandshape are used to quantify the number of graphene layers. Also the D ( $\approx 1350\text{ cm}^{-1}$ ) band, which indicates the presence of disorder, is a measure of the quality of the samples. For CVD grown graphene, the bandshape alone can no longer be used to identify the graphene layers due to a lack of order in the *c* axis. However the  $I_{\text{G}}/I_{\text{2D}}$  ratio provides a more suitable measure of the number of graphene layers.<sup>24</sup> After the aforementioned initial screening, a Raman scan of as-grown graphene on Cu foil was routinely used to determine film thickness, coverage, quality, and defect density in order to identify suitable candidates for transfer to glass slides or SiO<sub>2</sub>-Si substrates for further evaluation. Although the spectra collected from graphene on Cu contained a sloping background, the G and 2D peaks were still visible. In order to evaluate the uniformity of the graphene films, we transferred them from selected samples to glass slides and 300 nm SiO<sub>2</sub>/Si-substrates using PMMA method (see supporting information for details) for optical transmittance and spatially-resolved Raman mapping, respectively. We also checked the sheet resistance of our samples using a four-probe AC-resistance bridge and the Van der Pauw method. Fig. 1e shows a large scale (1 inch  $\times$  3 inch) PMMA/graphene sample with sheet resistance of  $550\ \Omega/\square$  as an example.

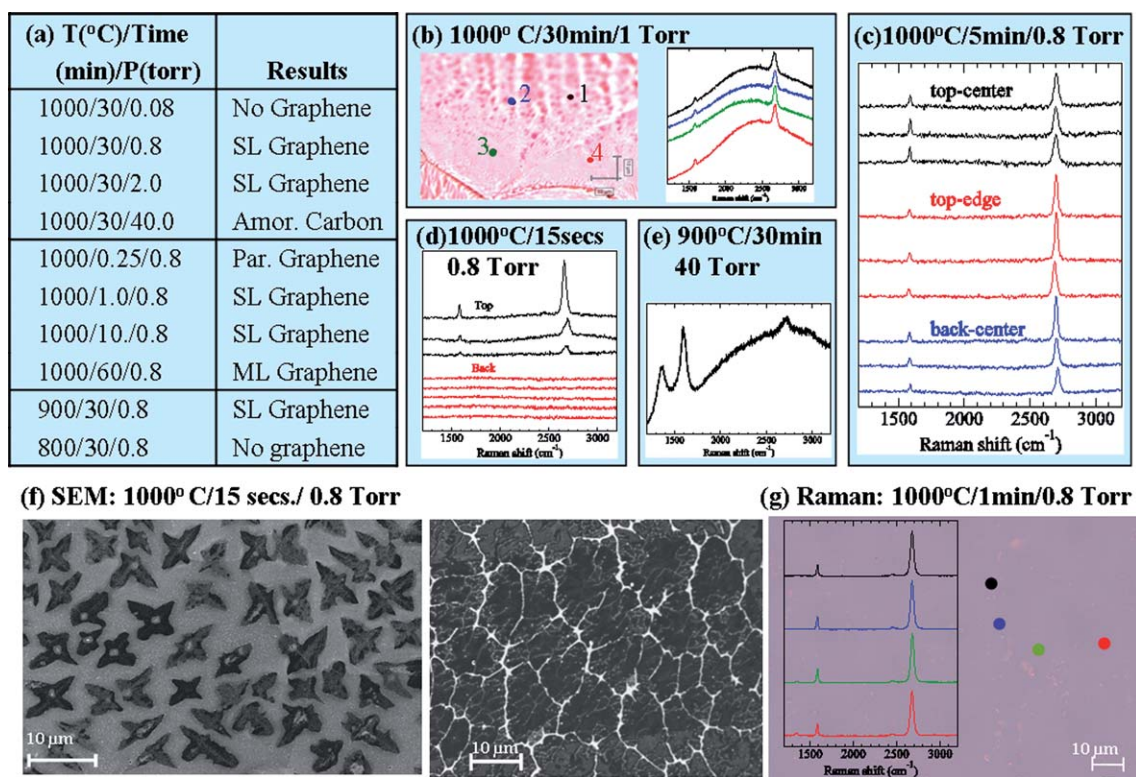
Fig. 2 summarizes the results for successful graphene formation from static methane vapor deposition. We obtained high-quality, large-area, single-layer graphene by simply exposing a hot copper foil to a given pressure of methane. Therefore, hydrogen and methane gas *flow* is not necessary for graphene formation. This may be intuitive as we are only growing one layer of carbon on the copper surface as opposed to gram-scale synthesis of fullerenes and nanotubes. We also studied the effect of temperature and methane pressure. The minimum temperature for graphene formation is around 900 °C. Above 1000 °C, copper sublimates and disturbs the formation of graphene. The best temperature is approximately 960 °C. Methane pressure also plays a critical role in the carbon deposition rate and graphene formation. At high pressures (such as 40 torr, Fig. 2e), we observe a Raman spectrum typical for amorphous carbon. The optimal pressure is  $\approx 1$  torr. When the methane pressure is low, the exposure time is not critical for single-layer graphene formation. The growth process is self-terminating as first suggested by Ruoff *et al.*<sup>15</sup> Interestingly, we found that it is a rather fast process; a 60 s exposure is sufficient to form a single layer of graphene as shown in Fig. 2. SEM images of 15 s exposure show partially-grown star-shaped graphene islands. This type of morphology has been observed in graphene prepared by the standard CVD procedures<sup>20</sup> and is attributed to the four-fold

nucleation and growth due to angularly dependent growth velocities on the [100]-textured surface of copper.<sup>20</sup> The second SEM image shown in Fig. 2 shows a fully covered portion of the as-grown graphene/copper sample with  $\approx 10$  micron graphene domains. These SEM images are very similar to the images of graphene synthesized by the standard CVD procedure<sup>13,15</sup> where the copper foil were first annealed under hydrogen flow and then followed by methane flow. Here we show that gas flow is actually *not* necessary and in particular one does not need to flow hydrogen to prepare the copper substrate. The last panel in Fig. 2g shows micro Raman spectra taken at different spots ( $\approx 2$  microns) of a PMMA-assisted transferred graphene sample, indicating the uniformity and high-quality, single-layer graphene formed with our safe, simple, “static” methane vapor exposure technique.

Eliminating hydrogen and methane flow simplifies graphene synthesis significantly. Nevertheless it is still desirable to eliminate methane completely. We have found that many common liquid carbon sources such as benzene and methanol can be used directly (without any hydrogen flow) to grow high-quality graphene films on copper. To the best of our knowledge, there have only been a limited number of studies<sup>18,19</sup> that use liquid carbon sources. Also, these studies were based on the standard CVD methods with hydrogen flow. As we demonstrate below, using methanol, we naturally produce H<sub>2</sub> along with CO and some methane during the thermal cracking of methanol over copper, which is enough to activate/clean the copper surface and grow graphene. We have tested a variety of different liquid carbon sources including methanol, ethanol, benzene, hexane, toluene, acetic acid, and acetone. Among these, benzene and methanol yield the best graphene samples. Below we discuss these two liquid carbon sources while the results from other liquid carbon sources tested are presented as supporting information.

Fig. 3 shows graphene formed *via* both static and dynamic vapor exposure of benzene. As seen in Fig. 3a, unlike methane gas, static exposure to benzene vapor does not yield good quality graphene. We speculate that this is due to very fast carbon deposition since each benzene molecule can deposit six carbon atoms on the copper surface. At high pressures, such as saturation pressure or 2 torr, we observe a Raman spectrum similar to that of amorphous carbon. At low pressures, such as 0.3 torr, we start to observe Raman spectra similar to graphene but with large defect peaks. The coverage is not uniform, as the spectra differ around the sample (see Fig. 3a). On the other hand, dynamic vapor exposure of benzene gives rise to high-quality graphene films as shown in Fig. 3. At pressures as high as 50 millitorr (flow rate  $\approx 0.2\text{ cc/h}$ ), we obtain uniform graphene coverage, but again with large defect peaks (Fig. 3b). Lowering the pressure down to 25 millitorr ( $\approx 0.06\text{ cc/h}$ ), we no longer observe any defect peak and the Raman spectra is typical of single layer graphene. Inspecting different regions of the as-grown graphene/copper foil indicates very uniform graphene coverage (Fig. 3c).

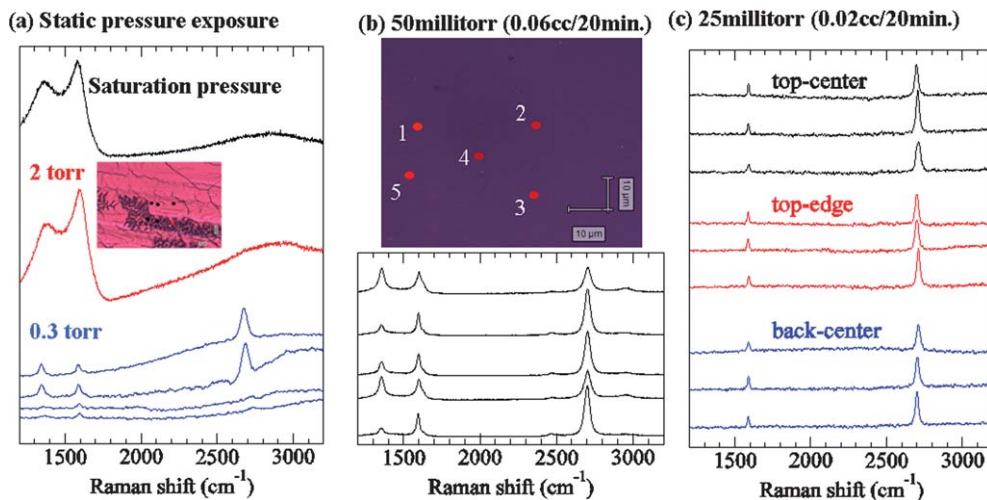
Graphene formation from methanol is very different from the other liquid hydrocarbons we studied because amorphous carbon formation was never observed (see Fig. S2). Over exposure to methanol vapor actually decreases the graphene formation. Hence, we find that there is a small sweet spot where a very high-quality, single-layer graphene forms from methanol vapor.



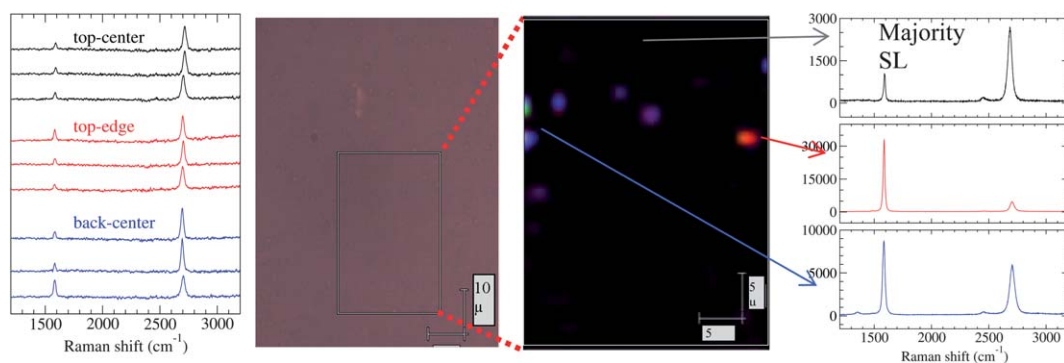
**Fig. 2** (a) Static methane pressure exposure CVD synthesis of graphene on copper substrate as a function of temperature, time, and pressure. SL, ML, and Par. indicates single, multi and partial layers, respectively. (b) Optical image of copper/graphene foil along with raw Raman data taken at four random spots. Note the large background scattering due to copper foil. (c) Raman spectra from various parts of the as-grown Cu/Graphene foil (after background subtraction). (d–e) Raman spectra from graphene/copper foil for different CVD conditions. Note that at high pressure we observe a spectrum typical for amorphous carbon. (f) SEM images of graphene/copper foil with 15 s. CVD synthesis, showing star-like graphene domains and fully covered regions with domain boundaries (white lines). (g) Optical image of a large area sample transferred onto a 300 nm SiO<sub>2</sub>/Si wafer and the corresponding Raman spectra at four random spots, showing uniform single layer graphene formation.

Fig. 4 shows graphene formed from dynamic exposure of methanol vapor, which yields high quality single layer graphene films. The optimum condition is determined to be 25 millitorr for about 10 min exposures. Exposures of more than 20 min degrade graphene formation and lead to non-uniform coverage. The

middle panel in Fig. 4 shows the optical image of a PMMA-assisted transferred sample and the corresponding spatially-resolved Raman map of G-peak intensity. The sample is mostly single layer graphene with only a few localized multilayer spots.



**Fig. 3** Raman spectra of graphene samples grown from benzene using static (a) and dynamic vapor exposure (b–c). Note that for static (a) and high-flow vapor exposure (b), we observe a Raman spectrum consistent with the formation of amorphous carbon or graphene with a significant defect peak. However for low pressure (c) exposure, we observe single layer graphene with uniform coverage.



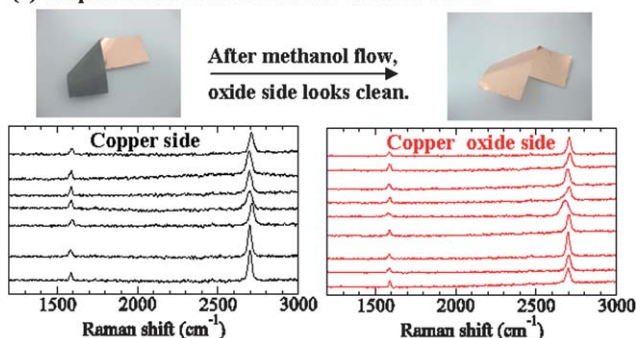
**Fig. 4** Graphene formation from low-pressure dynamic methanol vapor exposure. Raman spectra from different parts of the copper foil indicate uniform coverage (left). The middle panel shows the optical image of a transferred sample with spatially-resolved Raman mapping based on G-peak intensity, indicating mostly single layer graphene.

The results for graphene grown from methanol suggest that, unlike other hydrocarbons, methanol has a dual role; it is both the source of carbon atoms yet it inhibits amorphous carbon formation, possibly due to the production of OH-radicals. Similar results were also observed in methanol/ethanol synthesis of carbon nanotubes<sup>26,27</sup> where ethanol is used as the carbon source and methanol is used to reduce amorphous carbon deposition. At first glance, the C:H:O: ratio of 1:4:1 of methanol does not appear to favor carbon deposition. However, when the potential reactions that can occur over the catalyst are considered it can be seen that carbon deposition is thermodynamically favored.<sup>28</sup> Unlike gram scale synthesis of fullerenes/nanotubes, we seek a single atomic layer of carbon and a low carbon deposition rate is actually desired. However, if we wait for long times (more than 20 min), we accumulate various byproducts, such as H<sub>2</sub>O, OH-radicals, and CO<sub>2</sub> from the continuous thermal cracking of methanol that seem to prohibit additional carbon deposition. In the case of static exposure at long times (1 h to 3 h), we do not obtain much graphene on the copper foil. However, in the case of dynamic exposure, the byproducts were removed by the small flow of gas, and we obtain full coverage graphene/copper samples.

Thus far we have discussed graphene synthesis on bare copper foils where graphene actually grows on both sides of the foil. This is often not desired because graphene layers from the top and bottom surface of the Cu foil may combine during the etching process, yielding non-uniform, multilayer graphene films. Hence, it is desirable to develop a method which eliminates the graphene formation on one side of the copper substrate. Furthermore having a method to control graphene growth location on the substrate is important for patterned device applications. Our first attempt of controlled graphene growth was to synthesize graphene on one-side of oxidized copper foil (see Fig. 5a). We first oxidized the entire copper foil for one minute and then cleaned only one side with dilute HNO<sub>3</sub>. We hypothesized that graphene would form only on the clean copper surface. However, we found that shortly after methanol was introduced (between 1 min to 3 min), both sides of the copper foil were clean. Raman spectra show graphene formation on both sides (see Fig. 5). This demonstrates that methanol is a very good oxygen reducer due to hydrogen and CO formation during the thermal cracking of

methanol (see below). This explains why we do not need any copper activation or surface cleaning by hydrogen flow in our graphene synthesis. Methanol takes care of this naturally.

**(a) Graphene formation on one-side oxidized Cu foil**



**(b) Graphene formation on one-side CeO<sub>2</sub> coated Cu foil**

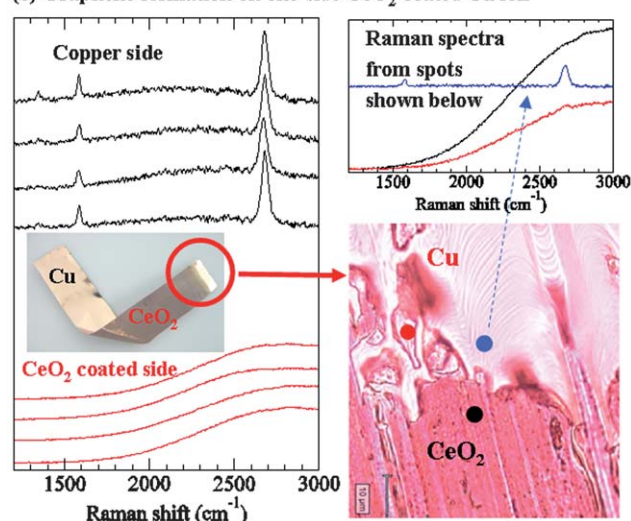


**Fig. 5** (a) Graphene formation on one-side of an oxidized copper foil from dynamic methanol flow. Note that after methanol flow, the oxidized surface is clean and both sides contain graphene. This suggests that methanol acts as a strong reducer, like hydrogen gas. (b) Graphene formation on a copper foil, one side of which was drop-coated with CeO<sub>2</sub>. Graphene forms only on the clean copper side. Right bottom panel shows the Raman spectra at three different spots near the CeO<sub>2</sub>/copper interface, showing graphene formation only on the copper surface.

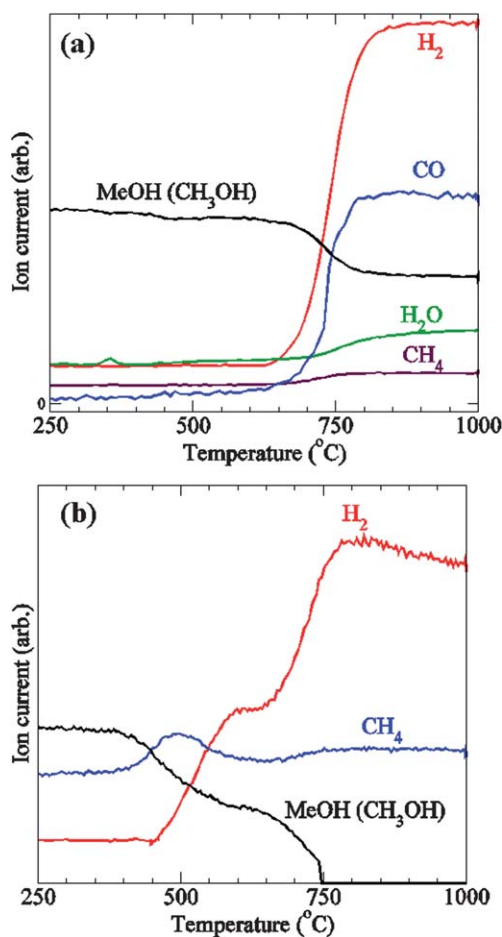


**Fig. 6** Mass-spectroscopy study of thermal decomposition of methanol over copper (a) and CeO<sub>2</sub> powder (b), respectively. Note that for copper powder (a), the methanol starts to decompose around 750 °C, producing hydrogen, CO, and trace amount of H<sub>2</sub>O and CH<sub>4</sub>. CeO<sub>2</sub> powder causes partial decomposition of methanol at 500 °C (b), releasing hydrogen and methane. At higher temperatures (~750 °C), methanol fully decomposes.

As a second attempt, we drop coated one side of the copper foil with CeO<sub>2</sub> by simply immersion one side of the copper foil in CeNO<sub>3</sub> based solution<sup>29</sup> (Fig. 5b). We note that CeO<sub>2</sub> has two functions; to catalytically decompose the methanol into hydrogen and methane, and to prevent graphene formation on the CeO<sub>2</sub> coated side. Indeed the Raman spectra of graphene grown on these foils, shown in Fig. 5b, indicate that we have graphene formed on the clean copper surface and nothing on the CeO<sub>2</sub> side. For high flow rates and thick CeO<sub>2</sub> coating, we observed amorphous carbon formation on the CeO<sub>2</sub> side. However during copper etching, the heavy and thick gray CeO<sub>2</sub> layer separates from the top layer of PMMA/graphene film and falls to the bottom of the etching solution, leaving single-layer graphene floating on the surface. Since CeO<sub>2</sub> coating is a simple electroless plating method,<sup>29</sup> one can easily coat any part of the Cu-foil with a given pattern with CeO<sub>2</sub> and thus the graphene film will grow opposite to that pattern. This is a very practical and useful finding for patterned graphene growth for device applications. More studies along these lines are in progress.

In order to gain a better understanding of the mechanism of graphene formation from methanol, we further studied the

thermal decomposition of methanol over copper and CeO<sub>2</sub> powder, respectively with mass spectroscopy (MS). The details of the MS measurements are given in the supporting information and our results are summarized in Fig. 6. Methanol starts to decompose over a copper surface around 750 °C, producing mainly hydrogen and CO. This helps to explain the strong reducing properties of methanol during synthesis. Both H<sub>2</sub> and CO can reduce the surface oxygen of CuO into Cu as was found in Fig. 5a. Also, we observe a trace amount of CH<sub>4</sub> and H<sub>2</sub>O production during the methanol decompositions. H<sub>2</sub>O, perhaps OH radicals, may assist in the observed amorphous carbon inhibition. The large amount of CO suggests that it may be the main carbon source for graphene formation. Carbon monoxide has been successfully used in the CVD synthesis of high-quality, single-wall carbon nanotubes with minimal amorphous carbon. However, for a detailed understanding, more experiments are required. The second panel in Fig. 6 shows the catalytic decomposition of methanol vapor over CeO<sub>2</sub> powder. The MS shows that the decomposition occurs in two steps. At 500 °C, the methanol partially decomposes into hydrogen and methane. At high temperatures, ≈750 °C, methanol fully decomposes. We note that despite the low temperature of methanol decomposition over Cu and CeO<sub>2</sub> (≈750 °C and 500 °C, respectively), we did not observe any graphene formation at these temperatures. We still need to go up to 900 °C to start graphene growth. This is probably not due to the thermal decomposition of the hydrocarbon molecules but rather because of the required surface diffusion necessary to form a uniformly covered graphene film on the copper surface.

We now discuss the determination of the number of graphene layers in our samples. Even though the Raman spectra shown in Fig. 2–5 are very convincing that we have single layer graphene, it is desirable to have another complementary technique to determine the number of graphene layers at centimeter scale (where Raman probes at the micron scale). Probably, the best measurement is optical transmittance which can give an overall average number of layers over a centimeter scale.<sup>30</sup> We transferred about 1.5 cm × 1.5 cm graphene films onto glass microscope slides to prepare samples with 1, 2, and 3 layers of graphene and measured the optical transmittance (Fig. 7) using ultraviolet-visible spectrophotometer (Varian Cary 50 Bio UV-Vis spectrophotometer). Our results agree with the values in literature, (≈2.3% absorbance per graphene layer<sup>30</sup> at λ = 550 nm). These data are easily reproduced from batch to batch (see Figure. S3a) and they all agree on the single layer value to within a half-percent. Therefore, we have produced single layer graphene from our simple methanol vapor without any hydrogen or methane flow. Very recently, it has been suggested that cooling rate can effect the number of graphene layers produced.<sup>31</sup> Motivated by this, we prepared samples with slow cooling (10 °C min<sup>-1</sup>) and air-quenched (≈200 °C min<sup>-1</sup>). However the optical transmittance data shows no significant difference (see Fig. S3b), and we always obtain single layer graphene from our methanol synthesis.

Fig. 7b shows the Raman spectra from 1, 2, and 3 graphene layers, which are all qualitatively the same with overall intensity increasing with layer number. Even though we observe the correct trend (G peak width and G/2D peak intensity ratio increasing with increasing number of layers), it does not resemble

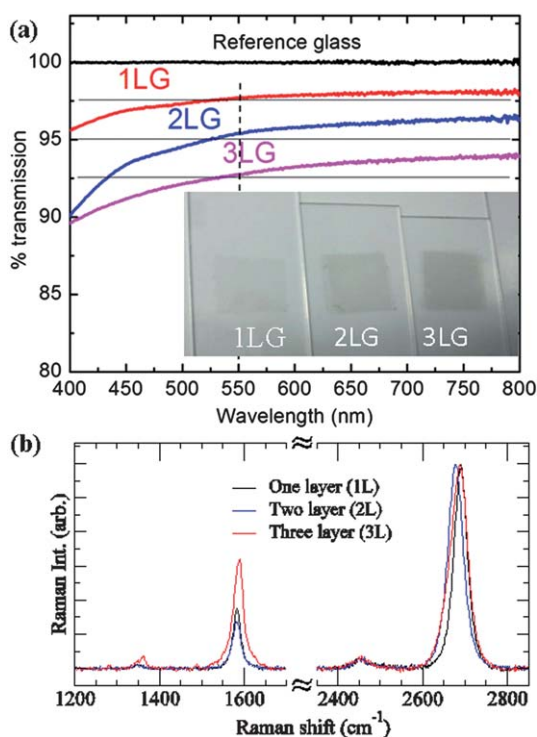


**Fig. 7** (a) Optical transmittance of large-area graphene films ( $\sim 2 \text{ cm}^2$ ) transferred onto microscope slides for one, two and three layer graphene. The horizontal lines show the average accepted values from literature. The bottom panel (b) shows the Raman spectra from the same samples. Note that the Raman G' or 2D band shape is not unique with graphene layer number due to random stacking.

the Raman spectra from Bernal stacked multilayer graphene samples. This suggests that due to the uncoupled nature of the individual graphene layers, randomly stacking them does not produce the coherent spectra obtained from natural multilayer graphene where each stack has well-defined AB orientations.

Finally, we measured the sheet resistance of our samples. Fig. 1e shows the image of a 1 inch  $\times$  3 inch graphene/PMMA film with a sheet resistance of  $550 \Omega/\square$ . This is consistent with values reported in literature<sup>25, 32</sup> for graphene grown with standard CVD methods. The fact that we get low sheet resistance over a three-inch square area graphene film further ensures that our safe, simple method produces graphene films as good as the standard CVD method.

### 3. Conclusions

In conclusion, we carried out a detailed systematic study of CVD graphene growth both from static methane vapor and a dozen of liquid carbon sources such as benzene and methanol. Our results can be summarized as follow:

- We showed conclusively that hydrogen annealing and methane flow used in standard CVD synthesis is not necessary for high-quality graphene formation. Graphene films can be prepared by a simply exposing a hot copper foil to a static low-pressure ( $\approx 1$  torr) methane vapor for a few minutes.

- The slow carbon deposition rate is found to be the key for high-quality graphene films. Fast carbon deposition (*i.e.* high

pressure or molecules with many carbons) yield graphene films with large defect peaks in Raman spectra and/or amorphous carbon films.

- We show that the best temperature for graphene formation is around  $900^\circ\text{C}$ . This is attributed to the required surface diffusion of carbon atoms rather than thermal decomposition temperature of the carbon source molecule. By using  $\text{CeO}_2$  catalyst on copper foil, we lower the thermal cracking of methanol to  $500^\circ\text{C}$  but still the high-quality graphene film forms only at temperatures  $900^\circ\text{C}$  or higher. The cooling rate was found to have no effect on the graphene film quality.

- We showed that the catalytic decomposition of methanol produces hydrogen, CO and methane, thus eliminating the direct use of the explosive gases,  $\text{H}_2$  and  $\text{CH}_4$ , in the graphene synthesis. Of over a dozen carbon sources studied, methanol is unique in that it acts as both carbon/hydrogen source and amorphous carbon inhibitor, regardless of methanol vapor pressure.

- Finally, we describe a method to limit graphene growth to a single side or selected location of the copper substrate, which is required for patterned device applications. Raman scattering, SEM, optical transmission and sheet resistance measurements clearly indicate that the samples produced with this safe and simple methanol method are of the highest quality.

### Acknowledgements

TY acknowledges partial support from DOE BES Grant No. DE-FG02-08ER46522. Work by IC was partially supported by the National Research Council. Research performed in part at the NIST Center for Nanoscale Science and Technology. We thank Dr Bulent Akgun for many fruitful discussions.

### References

- 1 A. K. Geim and K. S. Novoselov, *Nat. Mater.*, 2007, **6**, 183.
- 2 K. S. Novoselov, A. K. Geim, S. V. Morozov, D. Jiang, Y. Zhang, S. V. Dubonos, I. V. Grigorieva and A. A. Firsov, *Science*, 2004, **306**, 666.
- 3 K. S. Novoselov, Z. Jiang, Y. Zhang, S. V. Morozov, H. L. Stormer, U. Zeitler, J. C. Maan, G. S. Boebinger, P. Kim and A. K. Geim, *Science*, 2007, **315**, 1379.
- 4 A. K. Geim, *Science*, 2009, **324**, 1530.
- 5 F. Bonaccorso, Z. Sun, T. Hasan and A. C. Ferrari, *Nat. Photonics*, 2010, **4**, 611.
- 6 J. W. May, *Surf. Sci.*, 1969, **17**, 267.
- 7 A. E. B. Presland and P. L. Walker Jr., *Carbon*, 1969, **7**, 1.
- 8 F. J. Derbyshire, A. E. B. Presland and D. L. Trimm, *Carbon*, 1975, **13**, 111.
- 9 M. Elizenberg and J. M. Blakely, *Surf. Sci.*, 1978, **82**, 228.
- 10 J. C. Hamilton and J. M. Blakely, *Surf. Sci.*, 1980, **91**, 199.
- 11 C. Oshima and A. Nagashima, *J. Chem. Phys.*, 1997, **9**, 1.
- 12 J. Wintterlin and M.-L. Bocquet, *Surf. Sci.*, 2009, **603**, 1841.
- 13 C. Mattevi, H. Kim and M. Chhowalla, *J. Mater. Chem.*, 2011, **21**, 3324.
- 14 S. Bhaviripudi, X. Jia, M. S. Dresselhaus and J. Kong, *Nano Lett.*, 2010, **10**, 4128–4133.
- 15 X. Li, W. Cai, J. An, S. Kim, J. Nah, D. Yang, R. Piner, A. Velamakanni, I. Jung, E. Tutuc, S. K. Banerjee, L. Colombo and R. S. Ruoff, *Science*, 2009, **324**, 1312.
- 16 X. Li, Y. Zhu, W. Cai, M. Borysiak, B. Han, D. Chen, R. D. Piner, L. Colombo and R. S. Ruoff, *Nano Lett.*, 2009, **9**, 4359.
- 17 S. Bae, H. Kim, Y. Lee, X. Xu, J. S. Park, Y. Zheng, J. Balakrishnan, T. Lei, H. R. Kim, Y. Song, Y. J. Kim, K. S. Kim, B. Ozyilmaz, J. H. Ahn, B. H. Hong and S. Iijima, *Nat. Nanotechnol.*, 2010, **5**, 574.

- 18 A. Srivastava, C. Galande, L. Ci, L. Song, C. Rai, D. Jariwala, K. F. Kelly and M. P. Ajayan, *Chem. Mater.*, 2010, **22**, 3457.
- 19 Y. Miyata, K. Kamon, K. Ohashi, R. Kitaura, M. Yoshimura and H. Shinohara, *Appl. Phys. Lett.*, 2010, **96**, 263105.
- 20 J. M. Wofford, S. Nie, K. F. McCarty, N. C. Bartelt and O. D. Dubon, *Nano Lett.*, 2010, **10**, 4890.
- 21 Z. Sun, Z. Yan, J. Yao, E. Beitler, Y. Zhu and J. M. Tour, *Nature*, 2010, **468**, 549.
- 22 A. C. Ferrari, *Phys. Rev. Lett.*, 2006, **97**, 187401.
- 23 I. Calizo, A. A. Balandin, W. Bao, F. Miao and C. N. Lau, *Nano Lett.*, 2007, **7**, 2645.
- 24 I. Calizo, W. Bao, F. Miao, C. N. Lau and A. A. Balandin, *Appl. Phys. Lett.*, 2007, **91**, 201904.
- 25 A. Reina, X. Jia, J. Ho, D. Nezich, H. Son, V. Bulovic, M. S. Dresselhaus and J. Kong, *Nano Lett.*, 2009, **9**, 30.
- 26 S. Maruyama, R. Kojima, Y. Miyauchi, S. Chiashi and M. Kohno, *Chem. Phys. Lett.*, 2002, **360**, 229.
- 27 H. Qi, C. Qian and J. Liu, *Chem. Mater.*, 2006, **18**, 5691.
- 28 S. D. Jackson, D. S. Anderson, G. J. Kelly, T. Lear, D. Lennon and S. R. Watson, *Top. Catal.*, 2003, **22**, 173.
- 29 J. Edington, M. J. O. O'Keefe and T. J. O. O'Keefe, *Surf. Coat. Technol.*, 2006, **200**, 5733.
- 30 R. R. Nair, P. Blake, A. N. Grigorenko, K. S. Novoselov, T. J. Booth, T. Stauber, N. M. R. Peres and A. K. Geim, *Science*, 2008, **320**, 1308.
- 31 S. Lee, K. Lee and Z. Zhong, *Nano Lett.*, 2010, **10**, 4702.
- 32 Y. Zhu, S. Murali, W. Cai, X. Li, J. W. Suk, J. R. Potts and R. S. Ruoff, *Adv. Mater.*, 2010, **22**, 3906.
- 33 W. Zhou, H. Wu, M. R. Hartman and T. Yildirim, *J. Phys. Chem. C*, 2007, **111**, 16131.